Energy Harvesting for Wireless Sensor Networks

Vincent Lee

Electrical Engineering and Computer Sciences
University of California at Berkeley

May 30, 2012

Energy Harvesting for Wireless Sensor Networks

By

Vincent Chunwan Lee

A master's project report submitted in partial satisfaction of the

requirements for the degree of

Master of Engineering

in

Engineering – Electrical Engineering and Computer Sciences

in the

Graduate Division

of the

University of California, Berkeley

Committee in charge:

Professor Kristofer S.J. Pister
Professor Bernhard E. Boser

Spring 2012

Acknowledgement

In addition, I would like to take this opportunity to thank all of my past and present teachers, mentors, friends, and colleagues, who have made my experience and life much fuller. Thank you for their continual encouragement and support. Their friendship is deeply valuable to me, and their life lessons are worth its weight in gold.

Very dear to my heart, I wish to thank my mom, dad, sister, and everyone else in my family for their love, care, kindness, patience, and unfailing trust. Thank you for always being there for me. Mom, though you are not here to see the completion of my degree, I wish to dedicate it to you. Thank you so much for your unconditional support and love. I would not have the perseverance to continue facing everyday challenges without your continual and tireless devotion. Finally, I would like to thank the LORD, my God and Savior, for instilling in me the faith and courage to live each day by grace. Please take care of my mom in heaven, and thank You for giving me the strength to complete this degree.

Abstract

As energy demand, electricity prices, and carbon emissions continue to rise, there is a growing public desire to curb energy consumption to save money and the environment. According to Energy Star, "the average U.S. household spends $100 per year to power devices while they are off or in standby mode. On a national basis, standby power accounts for more than 100 billion kilowatt-hours of annual U.S. electricity consumption and more than $10 billion in annual energy costs". Based on PG&E's analysis, the wasted electricity produces 26.2 million tons of CO_2 each year in the U.S. Unfortunately, information in standard utility bills does not help consumers identify the culprit appliance responsible for their electricity waste, leaving consumers guessing for effective ways to save. Consequently, expensive hand-size devices, such as the Kill-a-Watt and Energy Hub, have emerged to identify energy consumption at a cost of ~$30 per outlet. The high cost and difficult installation of these devices limit their affordability and popularity. To address these issues, this work proposes a novel, plug-through power monitoring system for commercial and residential use. Our device detects any appliance's power consumption via a current sense transformer, which wirelessly couples magnetic energy from the appliance to output an electromotive force voltage. The voltage signal is relayed to the analog-to-digital converter of a GINA radio mote, which wirelessly transmits the data to laptops or smart phones via the Internet using 6LoWPAN wireless protocol. This allows consumers to view their real-time power usage from the convenience of their handheld device. The optimized design cost less than $5 to make and is easily installed, since the device never requires electrical contact with the outlet but is instead powered by scavenged magnetic energy, which charges an on-board storage capacitor. For a primary current of 12.6 A RMS, the device harvests up to 7 mW. Compared to present power monitoring devices in the market, our device boasts at least 6 times reduction in size and cost, serving as a disruptive technology to the power monitoring business while promoting more conscientious electricity usage.

1. Introduction

Electronics and electrical appliances have become an integral part of our everyday lives. From refrigerators to smart phones, almost every facet of our daily routine depends on some electrical device. However, we often overlook the amount of electricity required to sustain our habits. The standard monthly utility bill does not inform us how our daily decisions on electricity usage directly impact our monetary cost or our effects on the environment. In particular, the act of leaving electrical devices plugged into the wall outlet is a prime example. Even when electrical devices are turned off, passive power is continuously dissipated by them as long as they are connected to the electrical outlet. This leakage power is known as vampire power or standby power. According to Energy Star, "the average U.S. household spends $100 per year to power devices while they are off or in standby mode. On a national basis, standby power accounts for more than 100 billion kilowatt-hours of annual U.S. electricity consumption and more than $10 billion in annual energy costs" [1]. Based on Pacific Gas & Electric's (PG&E) analysis, this wasted electricity corresponds to 26.2 million tons of CO_2 released each year in the U.S [2]. If this wasted power can be mitigated or eliminated altogether, consumers will save significant monetary expenses as well as help improve the environment by reducing their carbon footprint.

In order for consumers to make informed decisions about electricity usage, they must first be provided with information or feedback on how their daily habits affect their energy consumption. Based on a study by the Department of Energy, 71 % of consumers were willing to change their energy habits when provided with information on their energy usage [3]. However, information in standard utility bills does not help consumers identify the culprit appliances responsible for their electricity waste. Thus, consumers are left guessing for effective ways to save.

This work explores approaches for helping consumers make informed choices about energy usage and recommends best practices to ensure consumers become more energy conscientious. In particular, this work will review various existing approaches to this problem, including their respective advantages and disadvantages. Then, this work will propose a novel solution to monitoring power, based on recent advances in microelectronics and wireless communication protocols. Technical aspects of the approach will be emphasized, including how current sense transformers and wireless sensor networks can be combined to achieve energy saving results. Comparison between the proposed solution and existing options, such as the Kill-a-Watt, will be made to highlight the advantages of this work. In addition, design considerations, constraints, and trade-offs of the proposed approach will be examined. Finally, areas for improvement and future work will be discussed.

2. Background

With continual transistor scaling due to Moore's law, the same electrical circuit several years ago can now be reproduced exponentially smaller at lower cost and with orders of magnitude lower power consumption [4]. Circuits which used to operate on 5 V have been redesigned to operate on ~1 V [4], allowing electronics to be completely powered by ambient energy. In addition, wireless communication technology has exploded in growth, allowing ubiquitous access to the Internet through Wifi, 3G, and other protocols. New wireless protocols have been pioneered, featuring reduced power consumption and increased robustness. Internet access is no longer limited to laptops or smart phones. As demonstrated by Dust Networks using the 6LoWPAN protocol, even the smallest environmental sensors can participate in the "Internet of Things" paradigm [5]. Combining these two advances establishes the technology necessary to develop wireless sensor networks completely powered by scavenged energy. Each sensor node

will no longer require the occasional battery replacement, thus extending their mean time between failures (MTBF).

Moreover, recent advances in wireless sensor technology have found numerous applications, ranging from mobile devices [6] to temperature sensors in a data center [5] or home [7], and from moisture sensors in the mountains [5] to current sensing of residential electricity usage [8]. In particular, this work will focus on power monitoring applications for residential and commercial use, where each node in the wireless mesh is associated to one outlet in the building and communicates via the 6LoWPAN wireless protocol.

For the moment, the current landscape for industrial wireless sensor networks consists of several major standardization efforts, including ZigBee (XBee), WirelessHART, Ultrawideband (UWB), 6LoWPAN, ISA100, and Bluetooth [9]. However, among those mentioned, only 6LoWPAN utilizes low power wireless IEEE 802.15.4 networks featuring IP version 6 (IPv6) [9], which allows each wireless sensor node to be assigned an IP address for communication over the Internet. Consequently, 6LoWPAN wireless sensors can be accessed anywhere in the world as long as internet connection is available; this cannot be said of sensors using other wireless protocols.

In terms of advances in energy harvesting, researchers have explored numerous ways to acquire sufficient power for these wireless networks, including photovoltaic, vibration, thermoelectric, and electromagnetic sources. A comparison of the various sources and necessary dimensions to acquire sufficient energy are summarized in Table 1, which is taken from [9]. Among those available, electromagnetic sources seems to be the most promising by allowing for sufficiently high energy densities.

Researchers at the University of South Carolina have demonstrated 10 mW of scavenged power from a 5-turn power cord with 13 A RMS of current flow [10]. Their energy scavenger consists of an open gap transformer core composed of many rolled-up layers of high

permeability MuMetal alloy (50 mm x 45 mm x 0.1016 mm), in order to capture the magnetic flux generated by the current flow. The energy in the captured flux is converted into an output voltage and current via 280 turns of copper coils on the secondary. A picture of their structure is provided in Figure 1. The acquired energy is sufficient to power most off-the-shelf low power wireless sensors. A comparison of some sensors is shown in Table 2.

Table 1: Comparison of energy harvesting techniques for wireless sensor networks from [9]

Energy Source	Performance	Necessary Dimension
Light (indoor)	$10 - 100 \ \mu W/cm^3$	$59 - 590 \ cm^2$
Airflow	$0.4 - 1 \ mW/cm^3$	$6 - 15 \ cm^3$
Vibrations	$200 - 380 \ \mu W/cm^3$	$16 - 30 \ cm^3$
Thermoelectric	$40 - 60 \ \mu W/cm^2$	$98 - 148 \ cm^2$
Electromagnetic Radiation	$0.2 - 1 \ mW/cm^2$	$6 - 30 \ cm^2$

Table 2: Comparison of off the shelf sensor platforms from [5, 9].
*Rx is receiving state. Tx is transmission state.

Features	XBee	SmartMesh IP DN6000	MicaZ	Mica2
Supplier	Digi	Dust Networks	Crossbow	Crossbow
Radio Frequency [GHz]	2.4	2.4 - 2.4835	2.4	0.90
Bandwidth [Kbps]	250	250	250	40
Current Consumption Listening / Rx / Tx [mA]*	-/40/40	0.01 / 4 / 9	8/20/18	8/10/17
Power Sleep [uA]	1	2	27	19
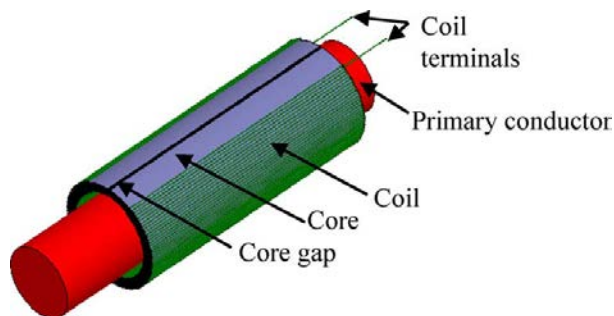
Figure 1: Multi-turn coil on a magnetic core that is wrapped around a current carrying conductor [10].

Unfortunately, several drawbacks of the design in [10] keep this harvester from being applied to power monitoring systems. For example, their harvester requires access to one of two wires making up a typical power cord, needs the conducting wire to be wrapped around the transformer core 5 times, and features a long form factor of 5 cm. This work will show how the form factor of the core can be reduced, while maintaining high levels of harvested power. By optimizing the transformer core design, the energy density of the scavenger can be increased through reducing core loss and decreasing the effect of the magnetizing inductance -- both of which are dimension dependent [7].

Currently, power monitoring options available to consumers do not employ these recent advances in wireless sensor networks or energy harvesting technologies. Conventional energy meter or smart meters [11] used by utility companies are large in size and only report collective energy usage, preventing consumers from knowing the breakdown of consumption on a per outlet resolution [11]. Some alternatives are available, but each has their own drawbacks as well.

One alternative is the Kill-a-Watt from P3 International [12] which interfaces between any appliance and the wall outlet. The device has an LCD display, which indicates real time energy usage in kilowatt-hours (kW-hr) and has the feature to translate this directly into monetary cost. However, each Kill-a-Watt retails for $30. In order to characterize energy consumption of an entire home, each outlet should have one of these devices. For example, if a home has 10 outlets, then the actual system cost is $300. For electricity usage up to Tier 2, 1 kW-hr cost $0.15 [11]. To recoup the cost of the Kill-a-Watt equipment, one must save 300/0.15 = 2000 kilowatt-hour, which can take roughly 3 years [11]. Other companies, such as Energy Hub and Powerzoa, offer similarly priced devices with the entire system costing over $300 [13, 14]. A summary of existing approaches to power monitor is provided in Table 3.

In all cases, the present monitoring products are not a viable solution due to large turnaround times to returns on investment or, in the case of smart meters, limited usefulness of

recorded information. From a technical standpoint, some mentioned devices have limited wireless capabilities, which do not allow them to be accessible via the internet [12, 13], hindering the convenience of their use and the report of feedback to users. Fortunately, due to recent advances in wireless sensor networks, all the mentioned drawbacks in power monitoring can be overcome, as will be shown.

Table 3: Comparison of power monitoring systems [12, 14, 15].

	Cost/outlet	Interface	Wireless Capability	Ease-of-integration
Kill-a-watt	$30	Screen on outlet	None	Plug into
Powerzoa	$30	Browser interface	Zigbee	Plug into
EnergyHub	$40	Central Hub with Screen, Browser	Zigbee	Plug into
Our goal	$10	Browser or smartphone	OpenWSN	Plug through (non-contact)

3. Methodology and Approach

Two approaches were conducted in creating our proposed power monitoring device. One approach aimed to use direct electrical connection from the outlet to power the device while the other aimed to use scavenged energy from magnetic flux. A general overview of the various modules needed for the power monitoring system is shown in Figure 2. Details on the direct connection approach can be found in the appendix as this paper primarily focuses on the energy harvesting solution. Nevertheless, in both approaches, the wireless communication system consists of the Guidance and Inertial Navigation Assistant (GINA) and GINA base station (Figure 3). Both are implemented by the Kris Pister Group at UC Berkeley. The board specifications and schematics are well documented and published on the OpenWSN website [16]. Though the GINA was built for navigation purposes, it was modified for this work to sample power consumption at the outlet and wirelessly communicate this information either

directly to the GINA base station or through a mesh network of GINAs before arriving at the base station. Upon receiving the signals from the GINA, the GINA basestation communicates via a computer to a remote server that displays the data in real time on a website: http://mengpowermonitor.appspot.com. This website can be accessed anywhere in the world as long as internet connection is available, allowing users to monitor their energy usage at will. The particular website choice is not important in this case, but simply demonstrates a proof-of-concept for this power monitoring idea.
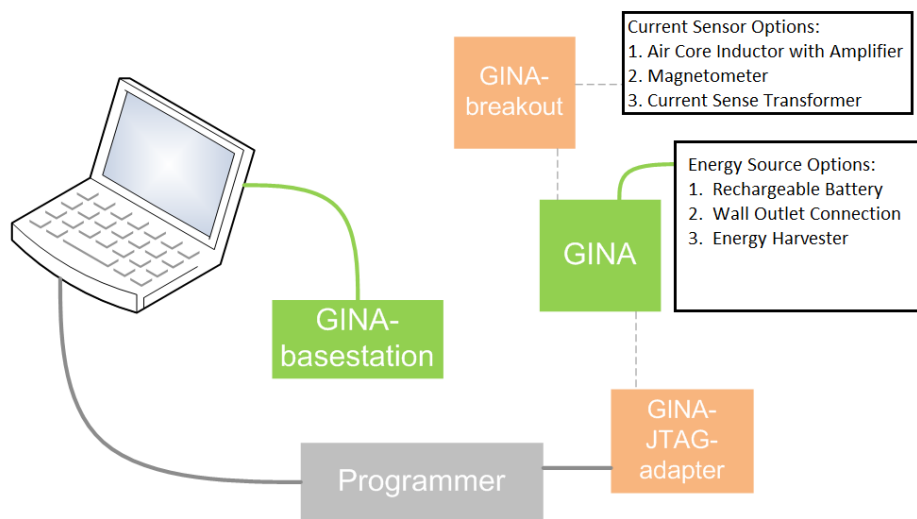
Figure 2: Overview of power monitoring system. Green: GINA boards used for wireless communication. Orange: Accessories for the GINA board. Breakout is an added board to spread out input/output connection pins. JTAG-adapter is used to program the microcontroller. Gray: Programmer for the GINA board. The actual power sensing is implemented by the current sensor, of which three options are considered. The energy source for the GINA is also listed, of which there are three options as well. Image is taken and modified from [16].
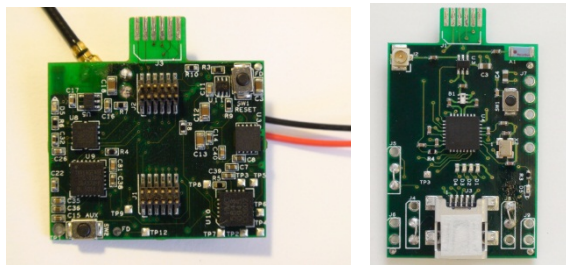
Figure 3: GINA board (left). GINA base station (right).

3.1. Power Supply Requirements

For the energy harvesting approach, all components should be adequately powered by the scavenger. Thus, specifications for power consumption must be determined. Since the GINA was not designed for the purposes of this work, many of the components are not necessary. Only the microcontroller with an analog-to-digital converter (ADC), radio, and antennae are the essential components. Other components, such as the LEDs, accelerometer, and gyroscope, were removed to reduce power consumption. As a result, the GINA consumes, on average, 1 mA of current at 3.3 V. Additional optimization can be done to further reduce power consumption, but this is beyond the scope of this work. Table 4 lists the power requirement that the energy scavenger must satisfy in this work. In addition, the power requirement for an optimal design is included for comparison.

Table 4: Power scavenging requirements for a) the GINA in this work and b) a future well-designed product. Note: GINA's average current usage is dependent on its communication settings, such as how often it transmits, etc. In this work, the GINA's setting was made to update the http://mengpowermonitor.appspot.com website every one to two seconds.

Modules	Power Consumption for This Work	Power Consumption for Optimized Design
Wireless Mote		
• **Average Usage**	1 mA x 3.3 V = 3.3 mW	10 uA x 1.5 V = 15 µW
• **Sleep Mode**	30 uA x 3.3 V = 100 µW	2 uA x 1.5 V = 3 µW
Sensor Circuit		
• Unity gain amplifier	81 uA x 3 V = 243 µW	0.33 uA x 1.8 V = 0.594 µW
Total Power Consumption	**3543 µW**	**15.6 µW**

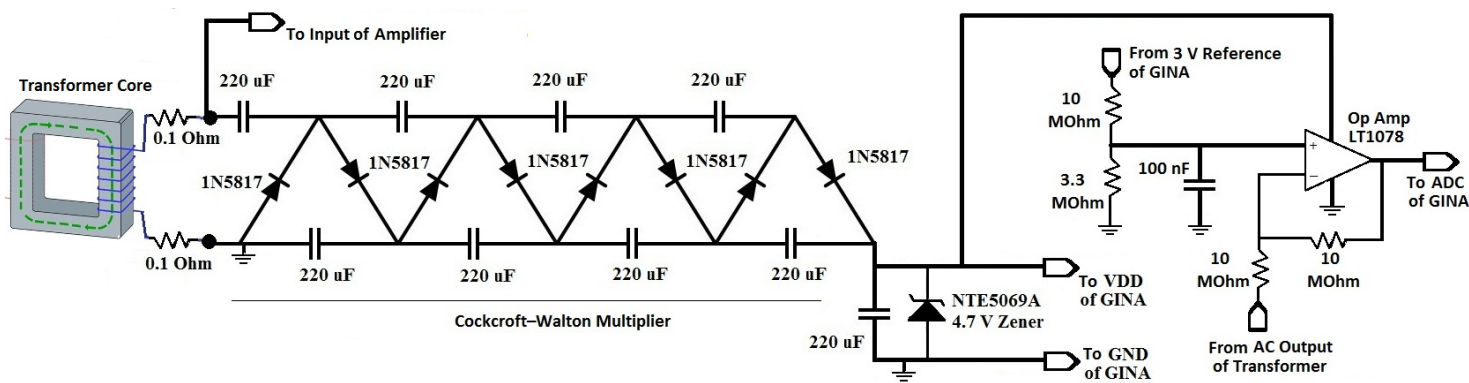### 3.2. Energy Harvesting Approach

The energy harvesting solution consists of the following components: a plug-through current transformer, 4-stage Cockcroft-Walton (CW) multiplier, storage capacitor in shunt with a Zener diode, and a unity gain amplifier. The current transformer serves as both the current sensor and energy harvester. The CW multiplier rectifies the AC output of the transformer and

feeds into the power supply of the GINA and amplifier. The amplifier buffers the transformer's AC output from the varying impedance of the GINA's ADC during switching and also DC biases the AC output for the ADC. Photograph of the prototype device is shown in Figure 4; corresponding circuit schematic is shown in Figure 5.
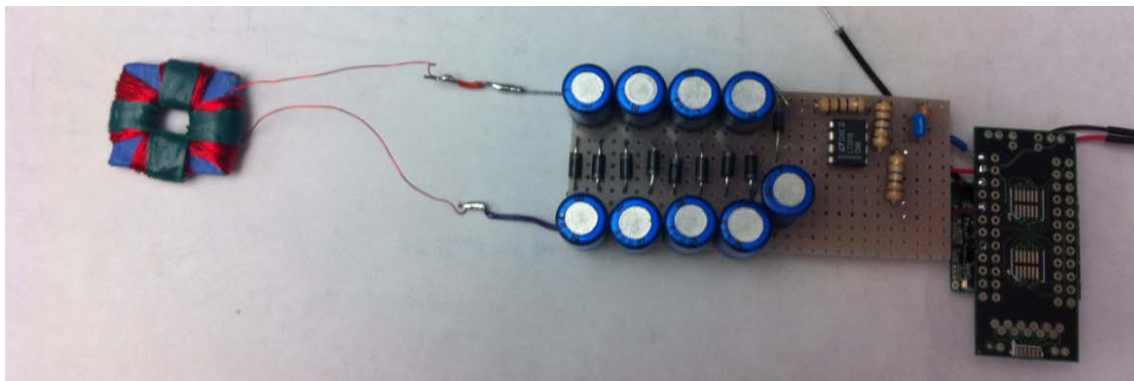
Figure 4: Photograph of prototype power monitoring device, based on energy harvesting approach.

Figure 5: Schematic circuit diagram of power monitoring device, based on energy harvesting approach.

3.3. Design of Transformer Core

The core dimensions design are restricted to the spacing of a typical household 120 VAC NEMA-5 outlet plug. The thickness of the core must be between 3 to 5 mm to fit between the plug and outlet. The metal width is determined by the prong separations on the plug, i.e. 5 mm. In addition, several materials are available for the metal core, including silicon steel (Arnon-5 [17]) or nickel-iron-molybdenum alloy (Co-Netic AA [18] or MuMetal [19]). In general, materials with higher permeability allow for larger output signal, and those with large saturation

field allows for a wider dynamic range of sensed current [20]. Arnon-5 has a relative permeability of 6000 with saturation field of 2.0 T, while Co-Netic AA and MuMetal have relative permeability up to 500,000 and saturation field of 0.8 T. The material properties are summarized in Figure 6 below.

Three types of transformer cores were built. Two cores were made by cutting up the metal sheets into "C" and "I" shaped pieces, which were then super-glued together and painted in insulating varnish. This procedure creates a finite gap at either the butt joint or overlap joint connection of the metal pieces. The third core is made by gluing together rectangular pieces of the metal and then drilling an opening in the center using a Dremmel tool. The core was then painted in varnish. This procedure allows for continuity in the metal but posed a greater construction challenge due to hardness of the metal and weakness of the glue during drilling. In all cases, the rough edges of the core was beveled and wrapped in tape to keep them from cutting the wires during the coil winding process. Either 34 or 30 gauge magnet wire was used to wind 500 secondary coils. Finally, the transformers were characterized using a HP 4192A LF Impedance Analyzer with the following settings: series circuit configuration, frequency at 60 Hz, and oscillation level at 0.2 V. A summary of the transformers is provided in Table 5 of Section 4.
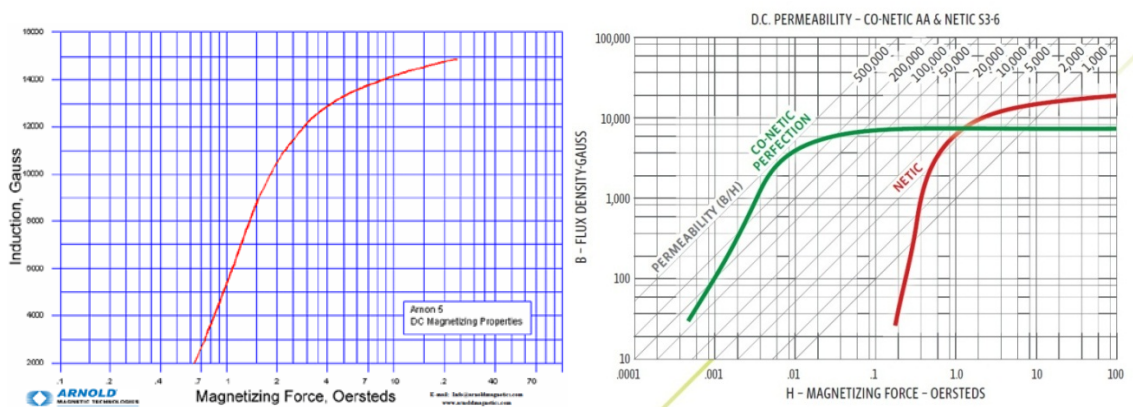
Figure 6: Flux density versus magnetizing force graphs for Arnon-5 (left) and Co – Netic AA (right). Note the relative permeability is defined as the flux density divided by magnetizing force.

3.4. Design of CW Multiplier

Due to low AC output voltages from the energy harvester, a Cockcroft-Walton design was chosen to rectify and boost the output voltage to usable levels. The design is based on the analysis in [21]. Equations 1 to 4 denote the steps of calculating the optimal capacitance to use in the CW, when given n stages, frequency f, output current I, and peak voltage Vmax of the AC signal. In our case, the following parameters were n = 4, f = 60 Hz, I = 1 mA, and Vmax = 1.25 V. Thus, the optimal CW capacitors are 225 uF. However, due to limitations of manufactured capacitor sizes, 220 uF was used instead.

$$\Delta V = \frac{I}{fC}\left(\frac{2}{3}n^3 - \frac{n}{6}\right) \tag{1}$$

$$V_{omax} = 2nV_{max} - \Delta V \tag{2}$$

$$n_{opt} = \sqrt{\frac{V_{max}fC}{I}}, \text{ for n} \geq 4 \tag{3}$$

$$V_{omax,opt} = \sqrt{\frac{V_{max}fC}{I}} \times \frac{4}{3}V_{max} \tag{4}$$

3.5. Design of Unity Gain Amplifier

The unity gain amplifier is powered by the energy harvester and serves as the interface between the AC output of the transformer and the ADC input of the GINA, which samples the waveform for processing. The LT1078 op amp was chosen because it operated at 3 V, which is very close to the GINA's voltage supply, and also consumes ~80 uA of supply current. At the positive input of the LT1078, 10 and 3.3 MOhm resistors were chosen to provide a 1.5 DC bias, while the 100 nF capacitor reduced effects of ripple in the supply voltage. At the negative input terminal, two 10 MOhm resistors are chosen to provide unity gain and reduce the current flow from the transformer's AC output to the GINA's ADC. The op amp output sums up the inverted AC signal from the current sensor with a DC offset of 1.5 V.

4. Results and Discussion

A no-joint transformer core was demonstrated to successfully power the GINA and an amplifier. With 12 A RMS on the primary, the AC output from the transformer is 470 mV RMS. The CW open circuit voltage reached 15 V, and a 4.7 V Zener diode was placed in shunt to clamp the voltage to avoid burning the GINA. With the Zener included, the CW stage can drive a 3.3 KOhm load with 3.5 V DC and 11 mV RMS ripple, implying a supply current of 1.06 mA DC and supply power of 3.7 mW. With the CW multiplier, GINA, and amplifier connected together, the CW output voltage dropped to 3.1 V due to higher than expected current draw, but the GINA remained operational and was able to wirelessly send packets to the basestation. Moreover, we found the current sensor's peak-to-peak voltage to be approximately linear with primary current.

4.1. Transformer Characteristics

Three types of transformers were created and measured. A summary of their respective features are provided in Table 5 below. Transformer I was made with 5 layers of Arnon–5 and features butt joint connections. Transformer II was made with 4 layers of 0.014 inch Co-Netic AA and features 0.6 x 0.6 cm^2 overlap joints. The joint overlap regions are 0.4 cm thick while other parts of the core are 0.2 cm thick. Transformer III was made of 3 layers of 0.014 inch MuMetal, stacked together using superglue with the center window cut out using a Dremmel. Thus, there are no core gaps in this transformer, unlike the previous versions. All three transformers have ~ 500 turns of 30 or 34 gauge magnet wires.
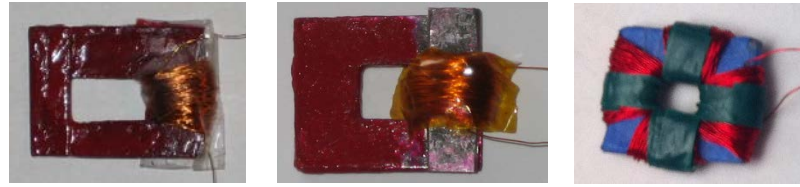
Figure 7: Three types of transformer designs, from left to right: Version I features Arnon-5 metal with a butt joint connection. Version II features Co-Netic AA metal with an overlapping joint connection. Version III features Co-Netic AA metal made without any joint connections.

Table 5: Summary of Transformer Core Designs.
Inductance and resistance were measured using a HP 4192A LF Impedance Analyzer.

Version	Structure Design	Material	Inductance (mH)	Series Resistance (Ohm)	Core Periphery (cm x cm)	Core Window (cm x cm)	Thickness (cm)	Wire Gauge
I	Butt Joint	Arnon – 5	5.2	6.1	2.9 x 1.9	1.7 x 0.7	0.3	34
II	Overlap Joint	Co-Netic AA	20	9.0	2.3 x 1.9	0.7 x 0.6	0.4	34
III	No Joints	Co-Netic AA	185	56.1	2.5 x 2.7	0.5 x 0.7	0.4	30

Explanation for the difference in inductance among the transformers can be attributed to the core gap size, as analyzed in [20]. The inductance is inversely proportional to the reluctance of the core metal and the core gap, as illustrated in Figure 8 and described by Equation 5. For the case where core gap is sufficiently large or the core permeability is high, the core gap reluctance will dominate and solely determine the performance of the transformer [20]. For the Arnon-5 material with relative permeability of 6,000 and mean path length of 6 cm, a gap greater than 10 um is sufficient to dominate the transformer characteristics. Theoretical calculations indicate transformer I should have inductance value of 0.8 H, but in experiments, the inductance was found to be 5.2 mH. This is attributed to the joint connections, which also explains why transformer I and II have lower inductance value than transformer III (i.e the no joint design). Transformer II has slightly better performance than transformer I because the overlap joint provided a larger cross sectional area at the gap. Nevertheless, for some unknown reason, transformer III has an inductance value less than the theoretical 3.4 H, despite using a no joint

design. The theoretical value can be calculated using Equation 5 and 7. Further investigation is required to understand the cause.
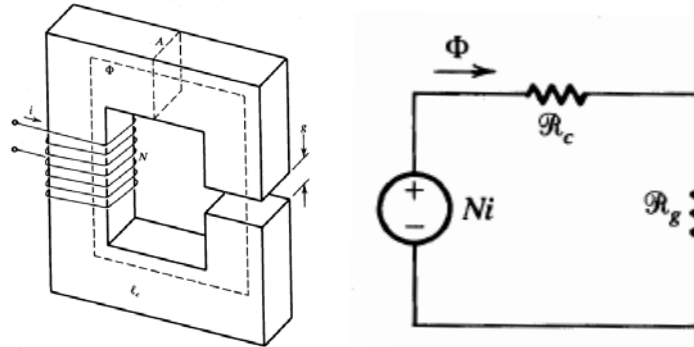
Figure 8: Illustration of a transformer core with a core gap (left). The flux is defined as Φ, A_g is the cross sectional area of the gap, A_c is the cross sectional area of the core, l_c is the mean path length of the flux, N is the turns ratio, g is the gap separation, and i is the current. The corresponding magnetic circuit is shown (right), where R_c and R_g are the reluctance of core and core gap, respectively. Images are taken from [20].

$$L = \frac{N\Phi}{i} = N^2 \left(\frac{1}{\mathcal{R}_c + \mathcal{R}_g}\right) = N^2 \frac{1}{\frac{(\mu_o/\mu_c)l_c}{\mu_o A_c} + \frac{g}{\mu_o A_g}} = N^2 \frac{\mu_o A_g}{g} \text{ for } g \gg \frac{l_c \mu_o}{\mu_c} \tag{5}$$

The transformers in all three cases can be modeled as shown in Figure 9, which consists of an ideal transformer in shunt with a magnetizing inductor L_μ and series resistance R_w [20]. Both of these parasitic components add loss and reduce the power harvested. Table 5 also has a summary of the measured L_μ and R_w values for each core. The $R_{connect}$ represents the connection resistance between the transformer and rest of the circuit, which is very small and typically 0.1 Ohm.
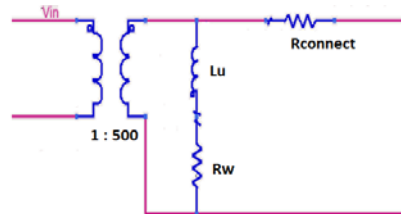
Figure 9: Model of transformer, including magnetizing inductance Lu, series resistance Rw, and connection resistance Rconnect.

The theoretical values for magnetizing inductance and leakage inductance are given by Equation 7 and 8, respectively. The leakage inductance was not included in the model because calculations based on given parameters in Table 5 showed they are much less than 1 mH. As indicated by Equation 7, larger permeability material results in larger magnetizing inductance. In the limit where µ approaches infinity, the transformer will become ideal.

$$L_u = \frac{N_2^2 A_c \mu_c}{lc}, \ L_l = \frac{\mu_o WLN_2^2}{3h} \tag{7, 8}$$

## 4.2. Performance of Energy Harvester

A comparison of the three energy harvesters is presented in Figure 10, which shows the scavenged power versus load resistance for the three transformer cores mentioned. Notice transformer III, which utilizes high permeability metal and lacks any core gaps, exhibits the highest performance in terms of harvested power. From Figure 10, there is an optimal resistance for peak power due the Maximum Power Transfer Theorem, which states maximum power is transferred when the load and source impedances are complex conjugates. In our experiments, we conducted impedance matching using a shunt capacitor for transformer II. The results are shown in Figure 11. However, the boost in power is not significant because of a low quality factor, $Q = \omega L/R = (400) (0.02H) / 9 = 1$. The same can be said of transformer III, where $Q = (400) (0.185H) / 56 = 1$. Additional results for transformer III is also shown in Figure 11, indicating scavenged power increases with increasing primary current, as expected from theory [20]. Note the peak scavenged power reaches ~7 mW when primary current is 12.13 A RMS. This power level is more than enough to power most wireless motes [9].

Further optimization of the design can provide even higher scavenged power. Notice the magnetizing inductance L_μ has a N^2 dependence while R_w only has an N dependence, where N is the turns ratio of the transformer. Thus, based on these equations, increasing the number of turns

will provide a higher quality factor. Consequently, impedance matching with higher Q values

will provide a voltage boost larger than 1, resulting in more power.
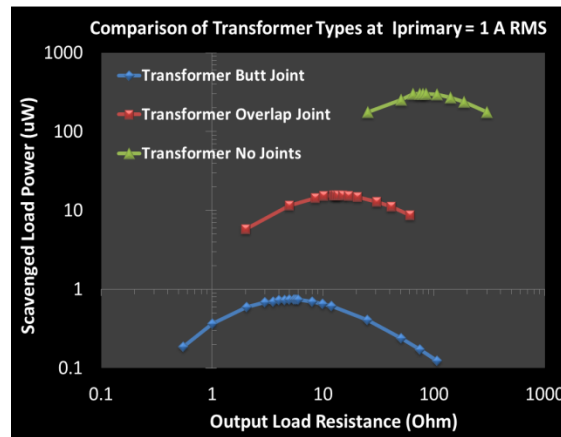
Figure 10: Comparison of energy harvester performance for three different transformer designs: butt joint, overlap joint and no joint designs. The peak in the curve results from optimal power transfer, when impedances are matched.
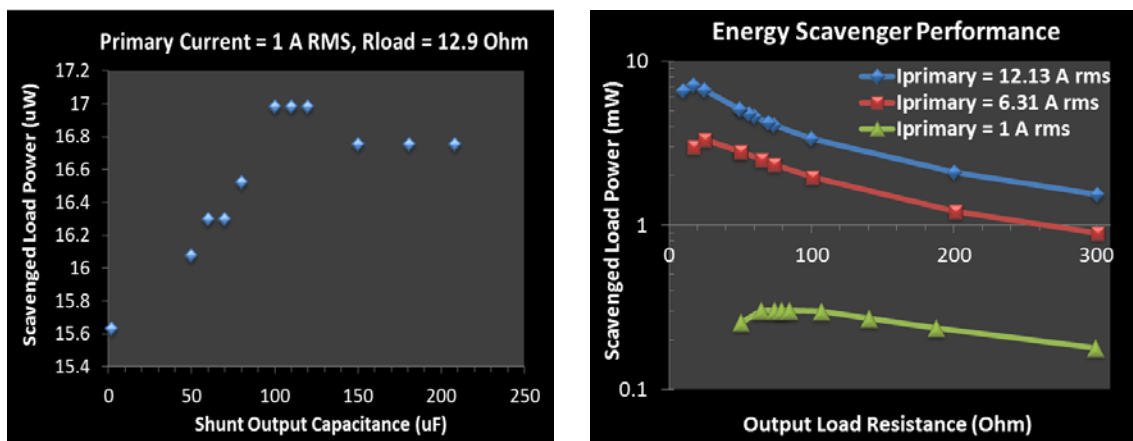
Figure 11: Scavenged power versus shunt output capacitance for transformer II. Measurements were performed using a 12.9 Ohm load and primary current of 1 A RMS (left). Scavenged power versus output load resistance for transformer III, performed at various primary current levels. The peak scavenged power slightly exceeds 7 mW for primary current of 12.13 A RMS (right).

Based on the model presented in Figure 9, Advanced Design System (ADS) simulations

were performed and compared to experiments. The model uses measured magnetizing

inductance and series resistance values from transformer III. The model and corresponding

results are shown in Figure 12. Simulation assumes a 60 Hz sinusoidal output voltage from the transformer, which results in higher calculated power than the measured values. As will be shown, a sinusoidal output voltage is not a correct assumption due to core saturation [20]. Also, the output load resistance that yields the peak harvested power is different between simulation and measurements. The model predicts an optimal load resistance of 86 Ohm, while measurement indicates 25 Ohms. Further inverstigation is required to understand if this discrepancy is also due to core saturation.
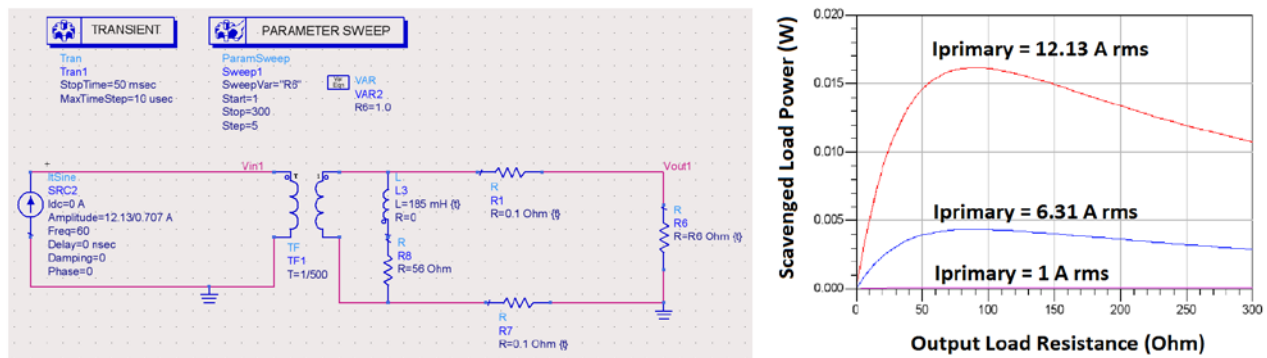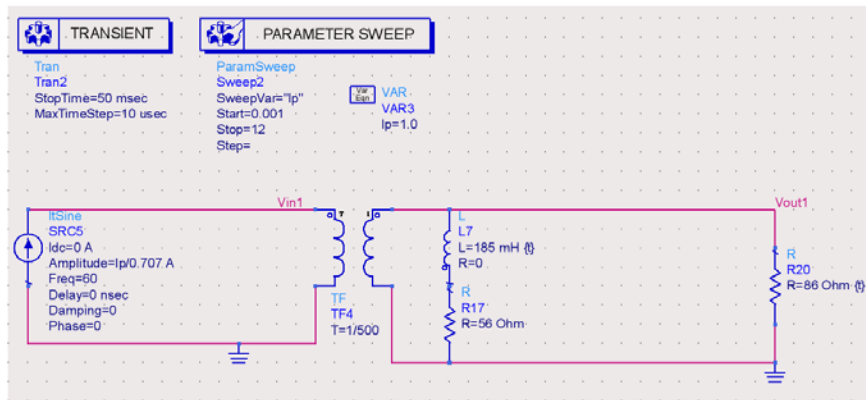

Figure 12: ADS model used to simulate transformer III (left). Simulation of scavenged power versus output load resistance (right). Notice the simulated scavenged power is higher than the experimentally measured values.

In addition, simulation and experiment results for scavenged power versus primary current were performed. The simulation setup is shown in Figure 13, and comparison between simulated and measured results is shown in Figure 14. The discrepancy in scavenged power at high primary current levels is due to core saturation [20]. Based on the data in Figure 14 and specifications in Table 4, a primary current of 0.375 A RMS is required to power a state-of-the-art mote, which consumes 15.6 µW. Since the energy harvester also serves as the current sensor, the power monitoring device can only sense current levels above 0.375 A RMS, which is still a useful amount of current to measure. An appliance drawing 0.375 A RMS from a 120 V RMS outlet is consuming 45 W. A study by the Lawrence Berkeley National Laboratory [22] had compiled a list of average power consumption for everyday devices. For example, an idle

computer desktop left on consumes 74 W, and a television when on consumes 186 W. Leaving the computer or television on and walking off to another room is a common habit that can be monitored with our proposed system. Consequently, users will be able to access this information and correct their behavior.

Furthermore, as transistors continue to scale due to Moore's Law and lower supply currents are needed, lower primary currents will be required to power the mote. Moreover, the results in Figure 14 are based on measurements from transformer III, which still has room for improvement.

Figure 13: ADS model of the energy harvester used to generate results in Figure 14.
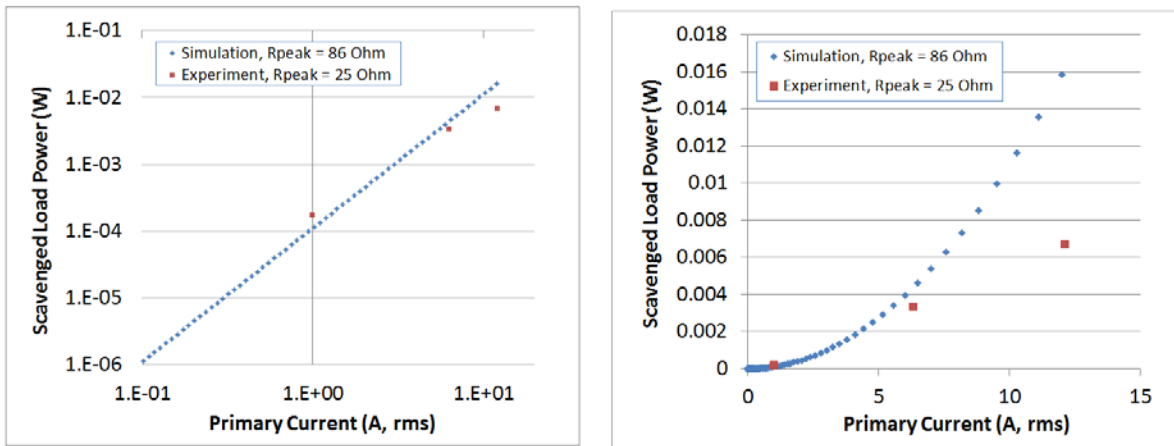
Figure 14: Measured and simulated results of scavenged power versus primary current for transformer III. Results use constant load resistances: 86 Ohm for simulation and 25 Ohm for measurements because each respectively maximized the harvested power for the simulated and measured cases. The discrepancy between 86 and 25 Ohm requires further investigation as previously mentioned. The left and right charts show the same data, but are plotted on different scales for clarity.

4.3. Performance of Current Sensor

As a current sensor, transformer III exhibits linear behavior for primary current levels below 5 A RMS: the peak-to-peak output voltage linearly increases with primary current (Figure 15, left). However, at higher current levels, the output voltage no longer follows a linear tread due to core saturation [20] and a non-sinusoidal output voltage results, like the one in Figure 15 (right). Consequently, the actual power is no longer quadratically depended on $(Vpp / (2\sqrt{2}))^2$ as assumed for sinusoidal waveforms, and true RMS values must be used in calculating power, which was done in this study. At higher primary current levels, the protruding voltage peaks become taller and narrower. In essence, the waveform shown in Figure 15 carries less power compared to a sinusoidal waveform with the same peak-to-peak voltage [20].
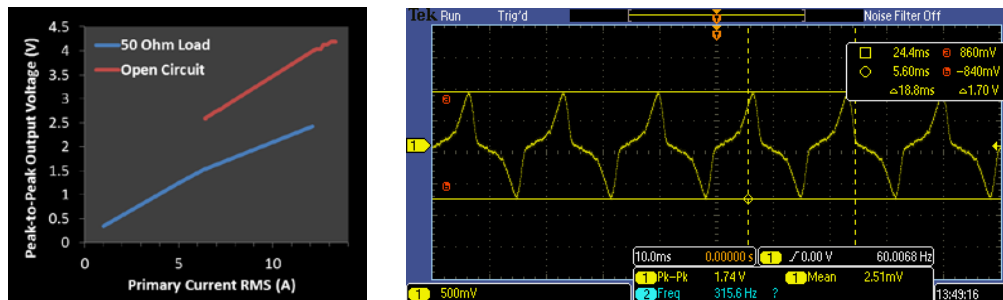
Figure 15: Peak-to-peak output voltage of transformer III versus primary current for various output loads (left). Output voltage waveform for transformer III exhibiting core saturation, when primary current is 6.31 A RMS (right).

4.4. Cost and Size of Power Monitoring Device

Overall, we achieved our goal by creating a smaller and lower cost power monitor device. The protoboard with on-board components is 0.7 x 3 x 1.5 cubic inches, while the Kill-a-Watt is 5.12 x 2.38 x 1.63 cubic inches [12]. Our prototype device boasts at least 6 times reduction in size. Of course, as a product, our board must be packaged to cover exposed components, possibly doubling its size in the worst case. However, even in that scenario, our prototype device is still 3 times smaller than the Kill-a-Watt and has wireless internet capabilities that no

other monitoring systems currently possess. Moreover, the cost to create our device is under $5, which is more than 6 times lower cost than the retail price of the Kill-a-Watt or Energy Hub solutions. With reduced cost due to economy of scale, some added cost from quality control, and a mark-up price for a profit margin, the overall product can still be sold for around $10 [23].

However, the cost and size can be further reduced by several folds if surface mount components are used instead. Table 6 summarizes the estimated cost in producing the prototype as well as the projected cost of the optimized final product. The prototype uses through-hole components while the final product should use surface mount elements. Projections for the final product is $2.26 and 2.5 x 2.7 x 1 cubic centimeter, equivalent to 10 times reduction in price and 45 times reduction in size compared to current market solutions.

Table 6: Estimated cost of energy harvesting power monitoring device, excluding cost of GINA. Prototype used through-hole components. Final product should use surface mounts. [24, 25]

Component	Quantity	Prototype: Cost/Component (Through Hole, $)	Prototype: Lump Cost ($)
10 MOhm Resistors	3	0.004	0.012
3.3 MOhm Resistor	1	0.004	0.004
220 uF Capacitors	9	0.038	0.342
100 nF Capacitor	1	0.030	0.030
1N5817 Schottky	8	0.054	0.432
NTE5069A Zener	1	1.070	1.070
LT1078 Op-amp	1	2.800	2.800
Magnetic Core & Wire	1	0.3	0.3
Total Cost			**$4.99**

Component	Quantity	Final Product: Cost/Component (Surface Mount, $)	Final Product: Lump Cost ($)
10 MOhm Resistors	3	0.0013	0.0039
3.3 MOhm Resistor	1	0.0013	0.0013
220 uF Capacitors	9	0.0738	0.6642
100 nF Capacitor	1	0.0555	0.0555
MMBD717LT1G Schottky	8	0.03837	0.30696
BZB84-C4V7 Zener	1	0.03995	0.03995
ISL28194FHZ-T7 Op-amp	1	0.88750	0.88750
Magnetic Core & Wire	1	0.3	0.3
Total Cost			**$ 2.26**

Conclusion

A novel power monitoring device has been proposed, featuring real-time energy management from any internet-connected computer or smartphone. The monitoring device readily connects to any standard US wall socket or plug and consists of a GINA board interfaced with a current sensor and power source. Power consumption information is relayed via a 6LoWPAN mesh network of identical devices to a GINA basestation, which then wirelessly transfers the data to a remote computer server. At any time, residential or commercial users can retrieve aggregate data on their power usage by simply connecting to the server over the internet. The optimized system is projected to be at least 10 times lower cost and 45 times smaller size, compared to present solutions in the market.

The proposed device features an energy harvester capable of scavenging up to ~7 mW of power with 12.6 A RMS of current flowing through the monitored load. Approximately, three milli-watts are enough to supply the GINA and even less for other lower power motes. Further investigation into higher permeability materials and transformer core geometry is necessary to increase the harvested power level. Overall, based on the proposed solution, the entire mesh sensor network does not require battery replacement, increasing the mean time between failures.

Though the GINA board was used as a proof of concept, it is not necessarily the optimal board for use in this application. Among the many components on the GINA, only the microcontroller with ADC, radio, and antennae are required. Future work includes designing a lower power communication board capable of being completely powered by scavenged energy. Additional investigation in network robustness is needed for insights into the quantity and placement of these devices within an average American home.

Overall, this work has illustrated the feasibility of implementing a wireless power monitoring system capable of delivering real-time energy usage data to any internet-enabled computer or smartphone. By closing the feedback loop between our daily habits and energy

usage, this work is a big leap forward in helping users become more aware of their direct environmental and economic impact. From being more informed, anyone can make sounder energy choices to better their livelihood and planet.

Appendix

A1. Direct Connection Approach

The direct connection design includes a one stage Cockcroft–Walton rectifier with Zener diode in shunt with the output capacitor, an air core current sensing inductor, and an amplifier interfaced to the ADC of the GINA. The circuit schematic is shown in Figure 16. Comparison of PCB design and final board is shown in Figure 17. The one-stage CW provides a power supply of 4.2 V and 1.4 mA, with less than 20 mV RMS ripple. Several options were considered when implementing the current sensor: an air core inductor with an amplified output or a Sentron Linear 1-Axis Hall IC, CSA-1VG magnetometer. In both cases, the output of these sensors is converted to voltage and sampled by the ADC of the GINA. The specifications for the ADC are documented at [16]. The magnetometer was not chosen in the final design because it typically requires too much supply power: 11 mA supply current and 5 V supply voltage, resulting in 55 mW power consumption. Alternatively, the chosen candidate is the air core inductor. However, the inductor's output voltage was too low to be sampled by the ADC on the GINA. Thus, it requires a low power amplifier, such as LT1078, to gain up the signal. The LT1078 uses a 3 V supply and consumes ~80 uA supply current. A trans-impedance amplifier circuit configuration was chosen for the inductor to convert its current signal to an output voltage.
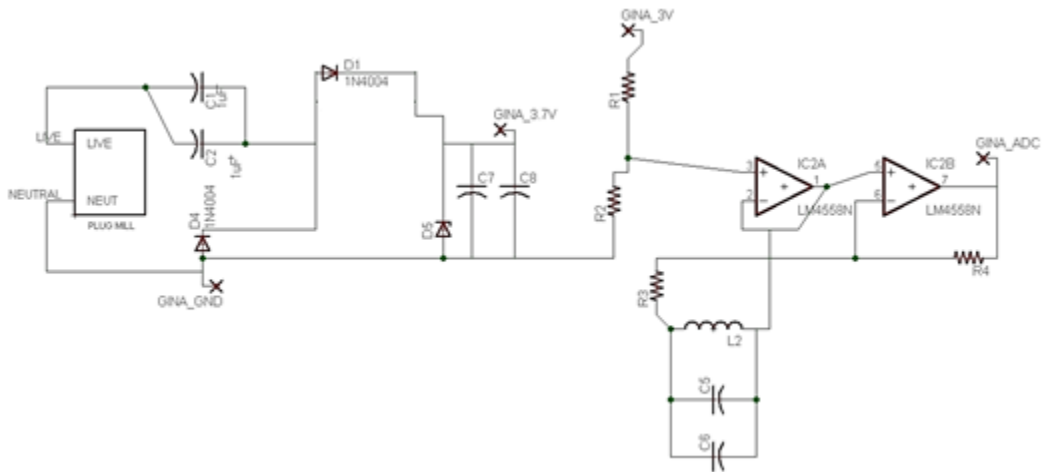
Figure 16: Circuit schematic for direct connection approach, featuring a one stage CW, a trans-impedance amplifier, and an air core current sensor. Note L2 is a sensor, measuring the magnetic field due to current in the wire.
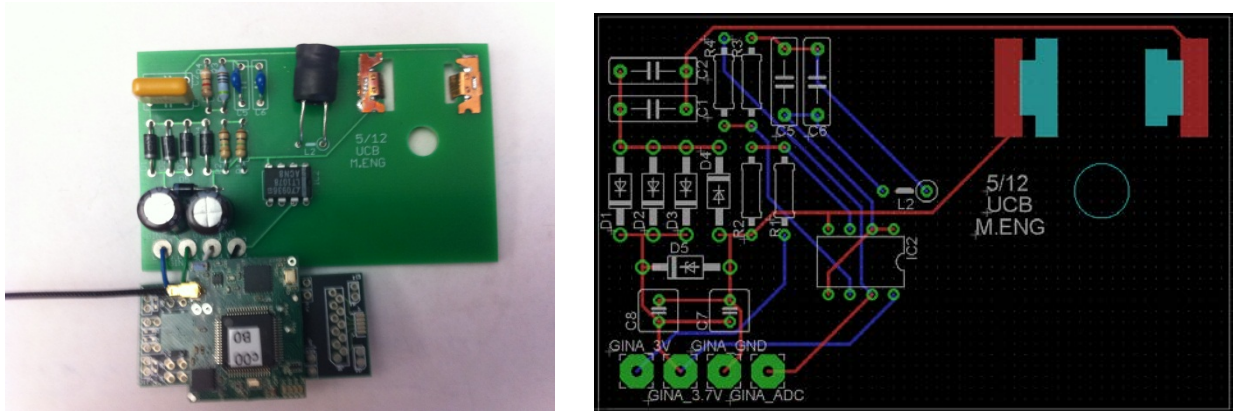
Figure 17: (Left) Photo of complete direct connection power monitoring device. (Right) Diagram of PCB board layout.

References

[1] Energy Star, "http://www.energystar.gov/index.cfm?c=about.vampires," vol. 2012, 2012, .

[2] PG&E, "http://www.pge.com/about/environment/calculator/," vol. 2012, 2012.

[3] Department of Energy, "http://energy.gov/," vol. 2012, .

[4] Y. Taur and T. H. Ning, *Fundamentals of Modern VLSI Devices.* Cambridge: Cambridge University Press, 2009.

[5] http://www.dustnetworks.com/products/smartmesh_ip, "Dust Networks," 2012.

[6] J. A. Paradiso and T. Starner, "Energy scavenging for mobile and wireless electronics," *Pervasive Computing, IEEE,* vol. 4, pp. 18-27, 2005.

[7] R. Moghe, Yi Yang, F. Lambert and D. Divan, "Design of a low cost self powered "Stick-on" current and temperature wireless sensor for utility assets," in *Energy Conversion Congress and Exposition (ECCE), 2010 IEEE,* 2010, pp. 4453-4460.

[8] D. Petersen, J. Steele and J. Wilkerson, "WattBot: A residential electricity monitoring and feedback system," in *CHI 2009, April 4 – 9, 2009, Boston, MA, USA,* 2009, .

[9] V. C. Gungor and G. P. Hancke, "Industrial Wireless Sensor Networks: Challenges, Design Principles, and Technical Approaches," *Industrial Electronics, IEEE Transactions on,* vol. 56, pp. 4258-4265, 2009.

[10] R. H. Bhuiyan, R. A. Dougal and M. Ali, "A Miniature Energy Harvesting Device for Wireless Sensors in Electric Power System," *Sensors Journal, IEEE,* vol. 10, pp. 1249-1258, 2010.

[11] http://www.pge.com/smartmeter/, "PG&E Smart Meter," .

[12] http://www.p3international.com/products/special/p4400/p4400-ce.html, "Kill A Watt," *P3 International,* .

[13] http://www.energyhub.com/socket/, "Energy Hub," .

[14] Powerzoa, "powerzoa.com/," vol. 2012, .

[15] Energy Hub, "www.energyhub.com/," vol. 2012, .

[16] http://openwsn.berkeley.edu/wiki/Gina#GINA, "Open WSN: Implementing the Internet of Things," vol. 2012, 10 March 2012, 2012.

[17] http://www.arnoldmagnetics.com/Non_Grain_Oriented_Electrical_Steel.aspx, "Arnold Magnetic Technologies Corporation," vol. 2012, 2012.

[18] http://www.magnetic-shield.com/products/alloys.html, "Magnetic Shield Corporation," vol. 2012, 2012.

[19] http://www.mushield.com/shielding-specs.shtml, "MuShield Magnetic Shielding " vol. 2012, 2012.

[20] J. G. Kassakian, M. F. Schlecht and G. C. Verghese., "Magnetic components," in *Principles of Power Electronics*, 1st ed.Anonymous Prentice Hall, 1991, pp. 565.

[21] C. L. Wadhwa, "Generation of high D.C. and A.C. voltages," in *High Voltage Engineering*, 1st ed.Anonymous Daryaganj, Delhi, IND: New Age International, 2007, pp. 56.

[22] Lawrence Berkeley National Laboratory, "http://standby.lbl.gov/summary-table.html," vol. 2012, .

[23] M. Mak, "Expert Interview
," vol. Staff Document Control Analyst, Global Product Data Management Group (GPDM) , Manufacturing Engineer, Advanced Micro Devices, Inc., March 10, 2012.

[24] Digi Key Electronics, "www.digikey.com/," .

[25] Mouser Electronics, "www.mouser.com/," .